

The 50 MeV cyclotron was operated through its final full year in the nuclear physics program on a normal seven day per week schedule with one or two shifts per week scheduled for maintenance. There was a scheduled shut-down for two weeks in June 1979 while the PDP 11/45 computer needed for certain experiments was sent away to be upgraded and repaired. Nuclear physics research with the cyclotron is scheduled to terminate in July 1979. After that time the cyclotron will be operated occasionally for testing components for the new cyclotron and for other intermittent needs which may arise during the next year or two, and which can be met without using the presently existing beamlines, since they will be dismantled. During the past year a high priority was placed on completing graduate thesis experiments and other research programs using light ions.

Those maintenance procedures necessary for keeping the accelerator in operation until the scheduled shut-down date were done. Improvements and new developments which would not pay off by then were not implemented, unless they were transferable to the superconducting cyclotron. For example, the vacuum has deteriorated from 8 μ torr to 20 μ torr due to the appearance of some leaks which are difficult to repair. The pumping system was also weakened when the roots blower ahead of the main roughing and backing pump wore out and was removed.

Since April 1979 the group developing the rf system for the K500 cyclotron has been given the use of the 20 kV DC anode power supply from the 50 MeV cyclotron whenever they need it. Operation of the cyclotron is not possible during these times, which are inserted into the schedule on a day-to-day basis. This procedure has allowed the rf development work to proceed at the maximum rate while giving 50 MeV cyclotron users the maximum possible use of the machine consistent with the high priority that the rf work has. The average fractional loss of cyclotron running time due to rf testing has been about 10% over a 3 month period.

Computer Control

Three projects using the PDP 11/20 computer and CAMAC interface to the cyclotron were completed. A program was written to log on demand the machine-readable control settings and power supply outputs. The log sheet that is printed has headings and spaces for writing in the information that is not readable by the computer, such as main magnet current, radio frequency, etc. The interface employs a 32-channel analog multiplexer and a high speed ADC for reading analog signals.

The multiplexer has been difficult to keep in working order, which has substantially hampered the use of the computer for data logging.

An automatic deflector conditioning program is in use. The program gradually ramps the voltage applied to the electrostatic deflector toward a specified final value and takes corrective action if the leakage current becomes excessive or other signs of sparking are detected. (See Fig. 1.)

A pair of electrodes for sensing the phase of the internal beam were installed in the dummy dee at $\theta = 0^\circ$ just inside the extraction radius. These were connected to the phase measuring system used previously with the intercepting phase probe. After some modification of the preamplifier and the computer program, this system was used in the feedback mode to stabilize the beam phase. Feedback control was via the computer to the current in the outer trim coil (number 8). Automatic phase stabilization is of great benefit when the superconducting magnet is being operated, as its fringing field can alter the field in the 50 MeV cyclotron by up to 3 gauss. Such large changes will detune the cyclotron, effectively shutting off the external beam. With phase feedback in operation the trim coil compensates for the changes in the applied field, and the cyclotron beam continues without any detectable change in the intensity on target.

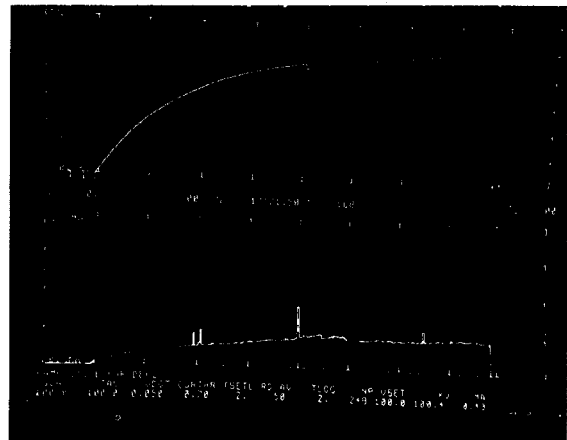


Fig. 1. Time dependence of voltage and current on the electrostatic deflector during an automatic ramp to 100 kV under computer control. The top graph displays voltage from 0 to 120 kV; the lower graph is the power supply output current consisting of deflector leakage plus the current flowing in the 398 megohm voltage divider used to monitor the voltage. The range of the graph is 0 to 2 mA. The time interval spanned by the horizontal axis is 600 seconds. Excessive current was detected at $t = 300$ sec. The program responded with a 4% voltage reduction.

In the proposed experiment to measure the parity-violating alpha width of the 0^+ , $T=1$ state of ${}^6\text{Li}$ at 3.56 MeV, a yield of ${}^6\text{Li}$ recoils from the $\alpha+d$ reaction is to be measured as a function of beam energy.¹ To ensure that the resonance due to this state is included in the region covered by the measurement, without unduly extending this region (and thus the data acquisition time), it is necessary to know the alpha beam energy (6.24 MeV) very accurately. Our aim is to measure this energy to 1 part in 10,000, by comparing the path of the beam in a magnetic spectrometer to that of heavy ions of the same rigidity from a surface ionization source. The energy of the heavy ions is to be determined from an absolute measurement of the voltage applied to the accelerating electrode of the source. Similar work is being done independently at the University of Auckland.²

In the surface ionization process, an atom (in our case thallium) of low ionization potential can be ionized by contact with a surface of high work function (in our case iridium) which is hot enough to thermally desorb the ion. Because of the surface nature of the interaction and the equipotential maintained by the metallic ionizer, the kinetic energy of the ions will be determined by the voltage applied to the ionizer. (The kinetic energies have a Maxwellian distribution characteristic of the temperature of the ionizer, but this is an effect at the 10^{-5} level).

A schematic diagram of the source is shown in Fig. 1. Thallium metal is evaporated from a tantalum boat placed inside a boron nitride oven, which is heated by current passed through tantalum wire. This atomic thallium passes through a hole in the convex ground electrode and is deposited on the 0.05 mm-thick iridium ionizer at the center of the concave high voltage electrode. The ionizer is indirectly heated by electrons from a tungsten filament at ground potential; its temperature is regulated by the emission current from this filament. Desorbed Tl^+ ions are accelerated through a hole in the ground electrode. The spacing and radii of curvature of the electrodes are chosen to obtain focusing of the beam at a distant point. The high voltage of 30.5 kV is supplied by a Spellman power supply which has high stability and a ripple of less than 0.001% RMS. The voltage is measured with a Julie Research Labs voltage divider, absolutely calibrated to 1 part in 10^4 , and a Hewlett Packard 3490A digital voltmeter. The accuracy of the voltage measuring system has been checked with a fluke 343-A DC voltage calibrator.

Currents of the order of $\ln\text{A}$ are obtained when the beam is collimated by a 2mm^2 aperture placed 30 cm from the source. No maintenance is required for periods of many hours of operation.

As one means of checking the absolute calibration of the ion kinetic energy, we have compared the rigidities of 6.051 and 6.091-MeV alpha particles from a ${}^{212}\text{Bi}$ source with that of the Tl^+ ions from the surface ionization source, using the MSU Enge split-pole spectrograph. Alpha particles were detected with photographic plates, and the position of the Tl^+ ion beam was measured both by scanning with voltage over the edge of the plate and by exposing the emulsion with the beam. The alpha particle energies have been measured with an accuracy of 0.1 keV by Grennberg and Rytz,³ who made length and field measurements in a magnetic spectrograph. Our first attempt resulted in a discrepancy of 2 parts in 10^4 , which is thought to be due to poor vacuum in the ion source chamber. A second measurement has now been made with improved vacuum; results are under analysis.

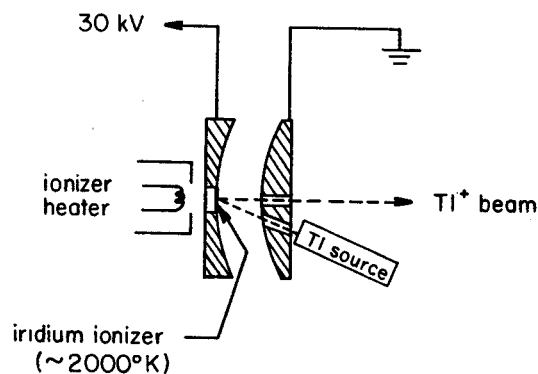


Fig. 1.

1. MSU Cyclotron Laboratory Annual Reports 1976-1977, 1977-1978.
2. P.H. Barker and R.E. White, private communication.
3. B. Grennberg and A. Rytz, *Metrologia* 7, 65 (1971).

Many of the experiments which utilize the Enge split-pole spectrograph rely on dispersion matching at the target. The dispersion matching is based on the ability to disperse the energy spread of the beam at the target so that it is cancelled by the dispersion in the spectrograph. This is accomplished by creating an image of Box 5 (Fig. 1) at the target with the magnification chosen such that the energy dispersion of the image will be cancelled by the spectrograph. This produces a well defined image at the spectrograph focal plane which, to first order, is independent of the energy spread of the beam. The magnification is adjusted by varying Q_8 , Q_{10} as shown in Fig. 1.

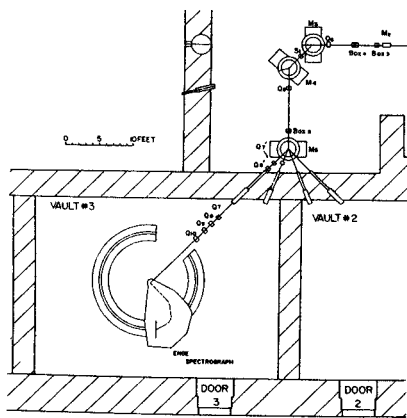


Fig. 1. Beamline layout illustrating focusing elements and bending magnets in relation to Enge split-pole.

The image produced at the target is the object seen by the spectrograph as in Fig. 2, which is considered transmission geometry. At scattering angles greater than 90° , transmission geometry becomes difficult to use, due to the effects of rotating the target. The target is normally rotated so that its angle is $1/2$ the scattering angle to minimize the effects of the beam spot centering on scattering angle and also to change the magnification at the target. For large target angles the horizontal size of the beam may be larger than extent of the target material being studied. For back angles, $\theta > 90^\circ$ it becomes beneficial to use a reflection geometry as in Fig. 3. In reflection geometry the object needs to be reversed so that the energy dispersion is in the opposite direction when compared to transmission geometry. To reverse the sign of the magnification a horizontal crossover in beam is required. With quadrupoles Q_7 , Q_8 , Q_9 , Q_{10}

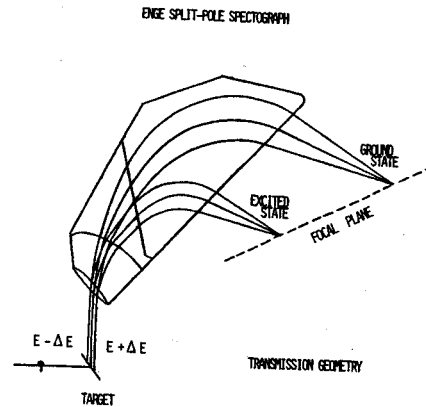


Fig. 2. Geometry used for forward angle dispersion matching.

this proved to be unfeasible due to their close spacing. Two additional quadrupoles were added to the beam line these being Q_7' and Q_8' in Fig. 1. Using Q_7 , Q_8 , Q_9 , and Q_{10} allows a horizontal and optionally, vertical crossovers between Box 5 and the target, having a large range of magnification. New quad settings were calculated for various horizontal magnification values using the computer code TRANSPORT. Typical spectra illustrating the results for transmission, and reflection geometry are seen in Fig. 4 and 5. Fig. 6 illustrates the result of no dispersion matching.

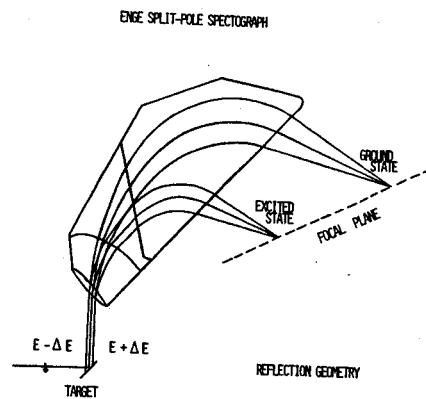


Fig. 3. Geometry used for back angle dispersion matching.

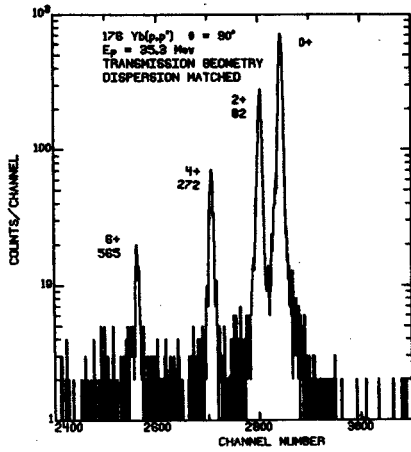


Fig. 4. Typical spectra resulting from forward angle dispersion matching (FWHM = 15 keV).

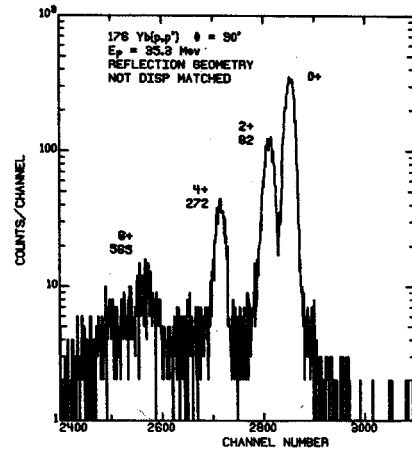


Fig. 6. Same target as in Fig. 4 & 5 but without dispersion matching.

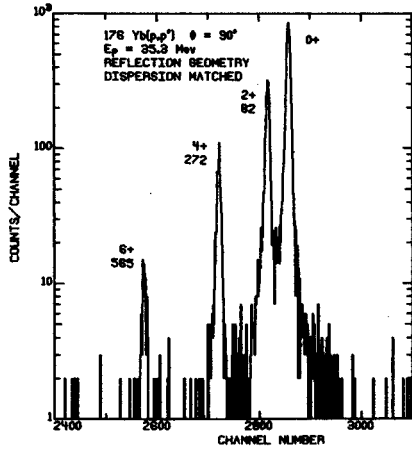


Fig. 5. Typical spectra resulting from back angle dispersion matching (FWHM = 15 keV).

An advantage of using the two quadrupoles near to the bending magnet M5 is that the beam is not allowed to get as large spatially which prevents the beam from scattering from the beam line. This is useful in reducing the background caused by scattered particles entering the spectrograph. An added result was that more beam could be transmitted to the target ($I=3, A$ for 35 MeV protons) which proved useful at the back angles where the cross section was low enough that the experiment was not count rate limited.

A gravity meter based on the Mössbauer effect has been proposed as a means to simplify and lower the cost of locating underground oil deposits by measuring gravitational anomalies.^{1,2} Feasibility studies on several isotopes with low energy metastable states led to the choice of ^{103}Rh for further work aimed at demonstrating the required gravitational sensitivity (1 ppm) in a gravitational red-shift experiment. Ranger Engineering Co. of Fort Worth, Texas is developing the gravity meter.

The primary source of radiation is produced by the $^{103}\text{Rh}(p,n)^{103}\text{Pd}$ reaction. All of the decays of 17-day ^{103}Pd produced this way lead to the desired 57-min ^{103}Rh metastable state. Natural rhodium is entirely composed of the desired isotope ^{103}Rh . The target was a circular section of a rhodium crystal, 2 mm thick and 6 mm in diameter. It was brazed to the water-cooled copper tip of the internal beam probe of the MSU 50 MeV cyclotron and bombarded with 12.7 MeV protons at a current of 90 μA . The beam fluence into the target during the first run was 4.2 coulombs. A second crystal prepared similarly and bombarded at 140 μA was overheated by the beam and melted, in rough agreement with calculations of the expected target temperature. A modified target has been designed in which the cooling water is applied directly to the back of the rhodium crystal. This target is expected to operate at 300 μA . A one-hour irradiation at that level will produce about 70 mCi of ^{103}Pd .

The immediate objective of this project was to produce a "cold" 40-keV ^{103}Rh source by Mössbauer activation with the cyclotron-produced "hot" 40-keV source. To this end, an unirradiated rhodium crystal was placed adjacent to the irradiated crystal. With recoil-free absorption in a perfect crystal, the Mössbauer activation would occur. The two crystals were placed in a liquid helium bath for several half lives. At liquid helium temperature the recoil-less fraction is rather high, 0.78, and the resonance shift due to the second-order Doppler effect³ is a million times smaller than at room temperature.

To demonstrate that activation occurred, we have only to count the activity of the previously "cold" rhodium crystal. In spite of the high activity of the source produced in the cyclotron and the long mean life for activation and counting, two effects severely reduce the expected number of counts. For one thing the 40-keV gamma ray is highly converted--only one in 1468 decays yields a 40-keV gamma ray. The

other effect is directly related to the long lifetime and narrow width, $\Gamma = 1.35 \times 10^{-19} \text{eV}$, of the resonance. The gravitational red shift, just barely observable⁴ with an ^{57}Fe Mossbauer source ($\Gamma = 4.7 \times 10^{-9} \text{eV}$), throws the absorption out of resonance for a height difference between source and absorber of only a few hundred Angstroms! This great sensitivity is, of course, at the heart of our interest in the project.

Nevertheless, after several experimental problems were solved, we had a run in which the expected number of K X-ray counts (from internal conversion) was around 5,000. Some the spectra, taken in a thin germanium detector, are shown in the figure. The top spectrum was taken during the time activation in a liquid helium bath was attempted. This is a background spectrum. The "activated" rhodium crystal was then counted during successive intervals. The resulting spectra are shown for the first two such intervals in the middle and bottom portions of the figure. Each of these intervals was one half life long, whereas the background was counted for almost 4 half lives. The 20- and 22-keV K_α and K_β X-rays from rhodium should appear in channels 91 and 102. As indicated on the background spectrum, there are indeed peaks at these pulse heights. However, their presence cannot be attributed to the rhodium crystal. For the most part all three spectra have the same shape and an intensity proportional to the counting time. We conclude that our failure to demonstrate Mössbauer activation was caused by imperfections in the crystals.

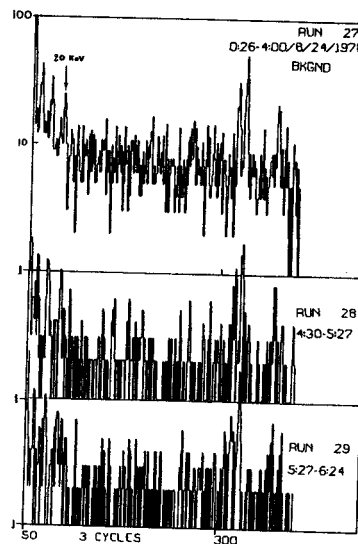


Figure 1

- † Present address: Lawrence Berkeley Laboratory
Berkeley, CA 94720
- †† Ranger Engineering Corporation, 3132 Bryan
Street, Fort Worth, TX 76110.
- ††† NASA Langley Research Center, Langley Station,
Hampton, VA 23365.
- 1. Jag J. Singh, NASA TM X-72703 (June 4, 1975)
NASA Langley Research Center, Hampton, VA
23665.
- 2. J.J. Spijkerman, J.J. Singh, D.H. Bohlen,
Kenneth H. Brown, R.A. Mazak, Proc. of Nassau
Mössbauer Conference (18 Nov. 76) Wynter and
Herber, eds. Nassau Community College Press,
Garden City, N.Y. (1977) 54.
- 3. R.V. Pound and G.A. Rebka, Jr., Phys. Rev.
Letters 4, 250 (1960).
- 4. R.V. Pound and G.A. Rebka, Jr., Phys. Rev.
Letters 4, 337 (1960).

The Multiwire proportional counter (MWPC) was further modified as proposed in the previous annual report with quite favorable results. The modifications included replacing the delay line making its total time delay 450 nsec (5 nsec/tap), compared with a previous length of 225 nsec, and the addition of new high voltage isolation and pulse transformers. The previously used ferrite pot core isolation pulse transformers were replaced with toriodal transformers. High voltage isolation was accomplished by winding the high voltage primary with wire encased in Teflon tubing (.75 mm O.d., .25 mm I.D.) on a Ferrite toriod¹ (6 mm I.D., 12 mm O.d., 5 mm thick). The secondary consists of enamelled copper wire wound on the toriod. To prevent damage to the insulation and to add some additional insulation, the toriod was wound with two layers of .125 mm Teflon prior to winding the primary and secondary leads. A turns ratio of 5:7 was used to achieve an input impedance of 50Ω to match the delay line impedance. The turns ratio was empirically determined by measuring the impedance of the transformer connected to the preamp as a function of frequency for a variety of transformer turn ratios and preamp impedances, and choosing the transformer-preamp pairing which gave 50Ω impedance over the desired frequency range while having a favorable voltage step up. It became apparent that the cable connecting the preamp to the transformers had an appreciable effect on the net impedance of the device, so that this had to be included in the test apparatus when doing the impedance measurements. The preamp impedance was chosen to be 110Ω which is much lower than the original 800Ω input impedance which used a 1:4 turns ratio. Both sets have a theoretical impedance of approximately 50Ω but the impedance of the cable which is about 100Ω tends to dominate if the preamp impedance is 800Ω thus greatly reducing the actual input impedance of the pair.

A change which greatly affected the operating condition of the counter was to reduce the diameter of the active wires from 0.0254 mm Tungsten to .012 mm double drawn stainless steel wires thus reducing the operating voltage required to obtain a specific gain.

Tests were made using 35 MeV protons from the MSU Cyclotron in the Enge split pole spectrograph, biasing the counter to 7000 V with 1/3 atm propane and methylal as the proportional gas. A spectra is seen in Fig. 1 for protons scattered from AuF_4 target. A comparison spectra is for the same reaction is seen in Fig. 2 with that

data being taken with the 25 cm inclined cathode delay line counter. The most noticeable aspect is the absence of wings, the high and low energy tails on the peaks in the MWPC spectra. In either spectra the resolution is 12-15 keV (.4 mm) FWHM which is well above the predicted resolution of .15 mm FWHM for the MWPC. However the resolution of the beam was not optimized during the test run. Various spectra for $^{238}\text{U}(p,p')$ and $^{197}\text{Au}(p,p')$ were recorded on-line with the program MULTIW by Ron Fox and event recorded on magnetic tape for analysis and playback at a later time. The on-line code, which exits in a machine language version is capable of data rates ≤ 1000 cps for the PDP 11/45 and does the complete position and angle calculation for each event.

A second experiment involving the MWPC was in conjunction with the 15N(3He,d)16O experiment of R.C. Pardo, R.G.H. Robertson and S.M. Austin. The principle of the experiment is to use a thick gas cell containing 15N gas and by using the angle readout of the MWPC, reject events which come from the windows of the gas cell. In this way the experiment may be done looking at only the reactions in the gas, thus getting rid of contaminant peaks.

The counter, biased to 7000 V using 1/3 atm of "Magic" gas (82.9% Ar, 16.85% Isobutane, .25% Freon) bubbled through methylal yielded an angular resolution of $.7^\circ$ which is nearly the predicted value of $.66^\circ$ FWHM angular resolution. Figure 3 shows some typical angle spectra. Figure 4 and 5 show spectra contrasting the effects of gating on angle to reject the particles scattered in the windows.

1. Ferrox cube. Type 3E2A. Ferrox cube, Saugerttes, N.Y. 12477

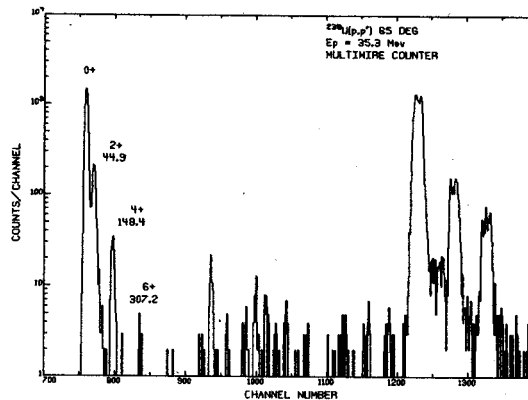


Fig.1 Position (energy) spectrum of protons scattered from natural UF_4 target.

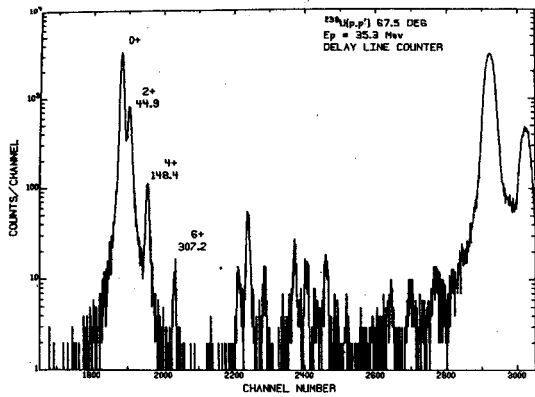


Fig. 2. Position(energy) spectrum of protons scattered from natural UF_4 target using delay line counter.

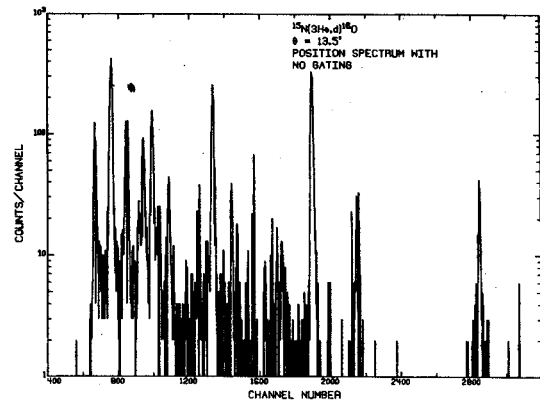


Fig. 4. $^{15}N(3He,d)^{16}O$ with no rejection of events from gas cell windows.

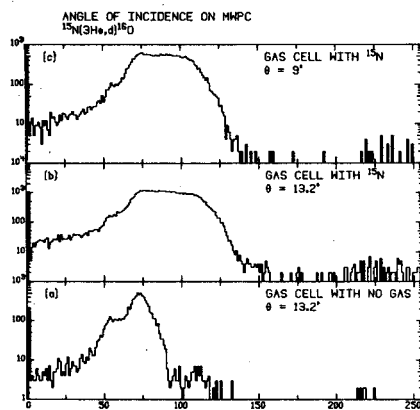


Fig. 3. Angle of incidence of protons on counter for three different configurations in the experiment. Angular range 35 → 55 deg.

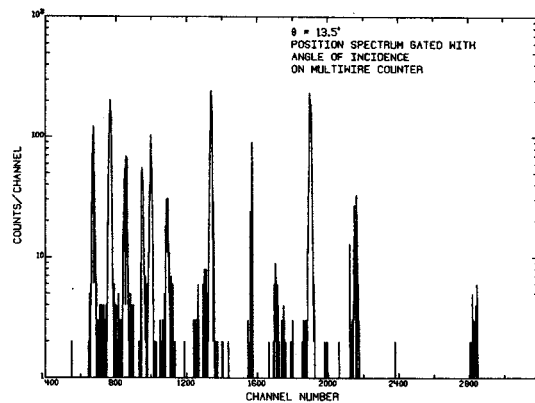


Fig. 5. $^{15}N(3He,d)^{16}O$ with rejection of events from gas cell windows.

Within the last year approximately 120 targets representing 60 different elemental compositions were manufactured in the MSU Heavy Ion Laboratory target making laboratory. While the majority of these targets required what is considered routine manufacturing processes (see table), a series of target requests for rare earth isotopic targets with $Z > 63$ were submitted requiring more sophisticated techniques. Targets of $^{168,170}\text{Er}$ and $^{154,156}\text{Gd}$ in particular were manufactured using an electron bombardment gun by first simultaneous evaporation and reduction of the oxides using thorium as a reducing agent. The reduced material was collected on a nearby water cooled copper condensing block, scraped free, and the metal re-evaporated to remove thorium contamination. The above process was based on techniques reported by L. Westgaard and S. Bjornholm.¹

Recent equipment work consists mainly of the redesign of the ion beam sputtering gun. The previous design utilized a modified ceramic electrical feedthrough as the gun's main body which required some machining and the addition of soldered fixtures for operation. The new gun, while using a similar operating design, substitutes a smaller cylinder of Dow Corning Macor machinable glass ceramic for the bulkier ceramic feedthrough allowing for bolt-on fixtures (see figure). Construction and cleaning of the new gun is done quickly

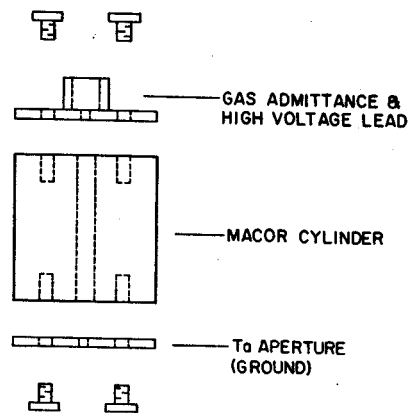


Fig. 1. Macor ion beam sputtering gun design.

and ease of machinability allows fast progressive modifications of physical dimensions for experimental optimization of gun performance. The extensive recyclability of the gun makes it most economical.

1. L. Westgaard and S. Bjornholm, Nucl. Instr. Meth. 42, 77 (1966).

Table 1. Representative list of targets manufactured.

Target Element	Chemical Form of Target	Starting Material	Method of Fabrication	Backing ¹	Thickness ($\mu\text{m}/\text{cm}^2$)	Amount of Isotope (mg) Required For 100 $\mu\text{g}/\text{cm}^2$
¹⁹⁷ Ar	Au	Au	Vacuum evaporation,	C	500	30
¹³⁸ Ba	Ba	BaNO ₃	Vacuum evaporation, ³ Ta point source, with Ta powder	C	≈ 100	20
²⁰⁹ Bi	Bi	Bi	Rolled	S.S.	5000	--
¹⁰⁶ Cd	Cd	CdO	Vacuum evaporation & ion sputtering	C	85	1
Ca/S	Ca/S	Ca/S	Vacuum evaporation, with dimple boat	C	200	--
¹⁶⁸ Er	Er	Er ₂ O ₃	Electron bombardment, Ta crucible with Th powder	S.S.	≥ 3000	15
F	CaF ₂	CaF ₂	Vacuum evaporation Ta point source	C	150	30
¹⁵⁴ Gd	Gd	Gd ₂ O ₃	Electron bombardment, Ta crucible with Th powder	C	150	10
^{6,7} Li	LiF	LiF	Vacuum evaporation with dimple boat	C	≈ 4	< 1
⁶ Li	Li	Li	Formed	S.S.	(1 cm)	(10 g)
²⁵ Mg	Mg	MgO	Vacuum evaporation, ³ Zr point source, ² with Zr powder	C	150	20
⁹² Mo	Mo	Mo	Ion sputtering	C	250	1
¹⁵ N	Melamine		Vacuum evaporation, with dimple boat	C	50	5
¹⁵ N	Uracil		Vacuum evaporation, with dimple boat	C	50	5
³⁵ Cl	NaCl	NaCl	Vacuum evaporation, Ta point source	C	150	20
²³ Na	Na	Na	Vacuum evaporation, with dimple boat	C	200	20
¹⁴² Nd	Nd	Nd ₂ O ₃	Electron bombardment	S.S.	250	5
²⁰⁸ Pb	Pb	Pb	Vacuum evaporation, with dimple boat	C	2000	20
S	S	S	Vacuum evaporation, with dimple boat	C	150	20
²⁸ Si	Si	Si	Electron bombardment	C	150	4
²⁹ SiO	SiO	SiO ₂	Vacuum evaporation, ³ Ta point source, with Ta powder	C	150	20
¹¹⁸ Sn	Sn	SnO	Vacuum evaporation, ³ Zr point source, ² with Zr powder	C	1000	50
¹⁴⁴ Sm	Sm	Sm ₂ O ₃	Vacuum evaporation, ³ Zr point source, ² with Zr powder	C	100	20
¹²⁴ Te	Te	Te	Vacuum evaporation, with dimple boat	C	1000	20
Th	Th	Th	Rolled	S.S.	850	--
ThF	ThF	Thf	Electron bombardment	C	100	30
²³⁸ U	UF ₄	UF ₄	Electron bombardment	C	100	1
¹⁷³ Yb	Yb	Yb ₂ O ₃	Vacuum evaporation, ³ Ta point source, with Ta powder	S.S.	5000	50
⁹⁰ Zr	Zr	Zr	Rolled	S.S.	20,000	--

1. S.S. refers to self-supporting targets and C usually means 20 $\mu\text{g}/\text{cm}^2$ carbon plus formvar.
2. Ta and Ar point source means tube with ends smashed and small hole drilled in its side.
3. Simultaneous reduction and evaporation.

This is a progress report on design considerations for a large heavy ion spectrograph to be used with MSU Phase II. A preliminary sketch indicating the position of the K = 800 spectrograph on the floor plan of the new heavy ion laboratory is shown in Fig. 1. Although the spectrograph design presented here is rather detailed, it is only intended to be suggestive and a focal point for discussion by the sponsors group and prospective users of the facility. Valuable input has been provided by K.L. Brown (SLAC), H.A. Enge (MIT), K. Halbach (LBL), S. Martin (Jülich), C. Morris (LASL), P. Roussel (Orsay), and H.A. Thiessen (LASL).

Because the accelerator has a non-zero energy spread ($\approx 0.1\%$) which is much larger than the desired experimental energy resolution ($\approx 0.01\%$), it is necessary to operate the system in the dispersion-matching or energy-loss mode. In this

mode the resolving power (D/M) of the beam dispersive or "beam analyzing" section is as important or more important than that of the spectrograph. An energy-loss system is shown in Fig. 2. In this example the dispersions are in the vertical plane and the beam dispersive section includes the two 45° bends on the left side of the figure. A phase space matching system consisting of a quadrupole quintet images the beam on the target and a QQDD spectrograph follows the target. The present example also includes a phase space rotator located in the first drift section of the beam dispersion system, labeled TWISTER (DRIPT) in Fig. 2. This quadrupole quintet interchanges the horizontal and vertical phase spaces when turned on, and is optically equivalent to a drift otherwise. (The quadrupoles are rotated 45° from the normal orientation.) Hence, the phase space rotation is optional and the choice is dictated by the particular

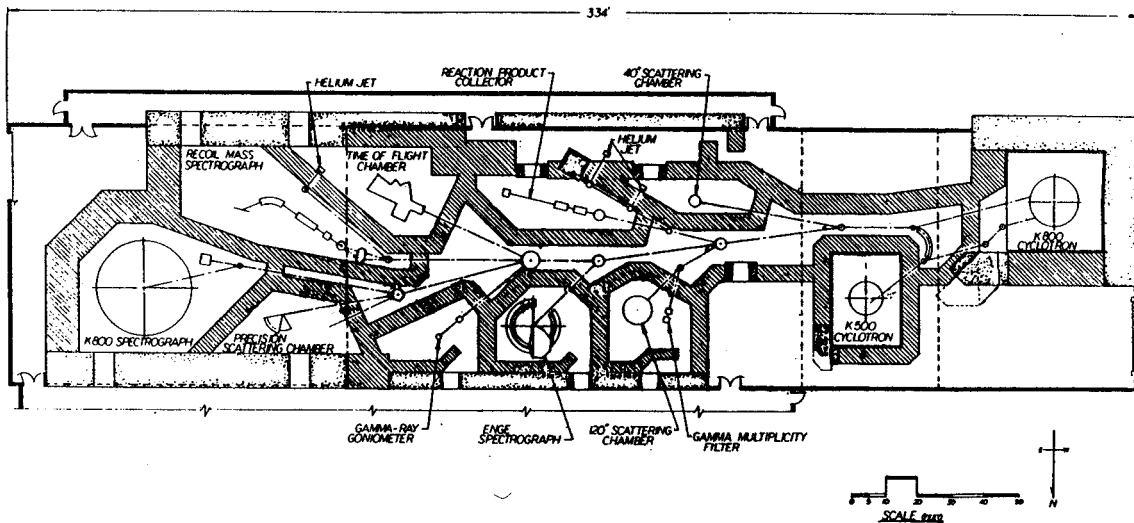


Fig. 1. Schematic plan view of the research facilities of the coupled superconducting cyclotrons at Michigan State University. The K = 800 spectrograph is indicated in the lower left hand corner.

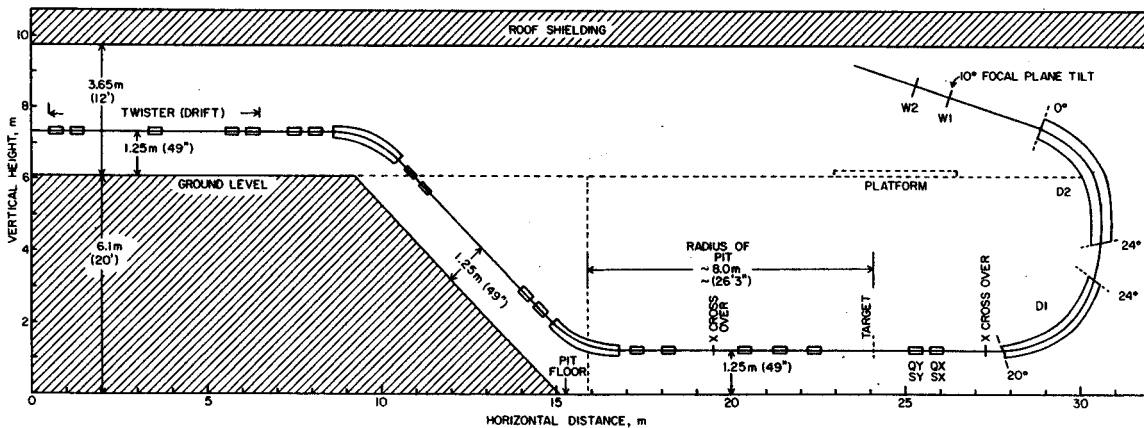


Fig. 2. An elevation view of a possible energy loss spectrograph system in the VHV mode.

experimental requirements. Typical phase space ellipse areas for the MSU superconducting cyclotrons are likely to be 1 mm-mr horizontally and 5 mm-mr vertically. With spectrograph dispersion in the vertical plane, better energy resolution is possible if the 1 mm-mr phase space is rotated into this plane. On the other hand, if angular resolution (measured horizontally) is the dominant experimental consideration, then it is best not to energize the TWISTER.

The choice of spectrograph mode, i.e., vertical (VHV) or horizontal (HHH), involves detailed consideration of reaction kinematics and angular resolution requirements and how they interact with the requirements for good energy resolution. The essential difference is that in the VHV mode the scattering and dispersion measurements are essentially decoupled with the former being in the horizontal plane and the latter in the vertical, while in the HHH mode the measurements are inherently coupled since both are in the same plane.

In the VHV mode the spectrograph optics are parallel-to-point in the axial direction and point-to-point in the radial or dispersive direction. Hence, the detector must be two-dimensional with momentum and scattering angle information being read out in orthogonal directions. A schematic view of the focal plane of such a system is indicated in Fig. 3. The scale and the reaction lines indicated are for the spectrograph to be described below and indicated at the right hand side of Fig. 2. Kinematics effects manifest themselves as tilted lines on the detector so that no focal plane motion or quadrupole tuning is required as the kinematic parameter changes with scattering angles. The focal plane momentum calibration also varies with kinematic compensation in the HHH mode, but is invariant in the VHV mode. It is also possible to observe sharp lines from several kinematically different reactions simultaneously.

It seems that simplicity of the tuning and the invariance of the focal plane calibration in the VHV mode are strong points in its favor. This simplicity is particularly important in a system which is to be used by a large number of different research groups. The two-dimensional focal plane detector of the VHV mode is a slight complication, but the HHH mode requires a minimum of two one-dimensional detectors and trajectory reconstruction to extract the scattering angle in comparable detail.

The QQDD spectrograph shown here is a combination of the QQDQ "Big Karl" system at Jülich and the QDD "HRS" system at Los Alamos. The design is not complete at this time but optics calculations with second order corrections do indicate that the principal design goals can be achieved with such a system. Detailed ray tracing

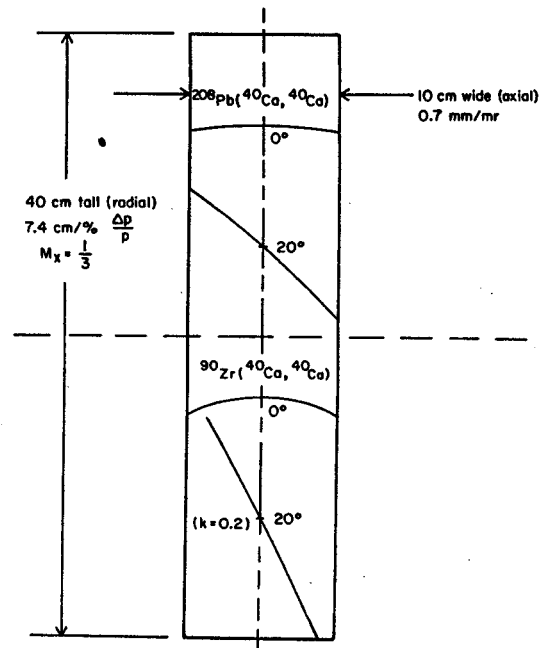


Fig. 3. Schematic view of the two dimensional focal plane of the proposed K = 800 spectrograph. The kinematics effects for elastic scattering of ^{40}Ca beams from ^{90}Zr and ^{208}Pb targets are indicated.

calculations will be carried out to determine the extent of higher order aberrations. The design of the superconducting quadrupoles and dipoles with superconducting windings will be initiated after a first order design is agreed upon. The present second order solution involves sextupole components in both quadrupoles as well as on the first, second, and fourth dipole edges. There is an axial waist between the two dipoles so that residual radial second and higher order aberrations can be tuned with an active multipole element at this location with minimum coupling to axial aberrations. The relatively large total bend angle of 161° was chosen partially to help keep the height of the system reasonable. Plots of the radial and axial beam envelopes through the QQDD spectrograph are shown in Fig. 4. The parameters of the spectrograph are listed in the table.

*Condensed from a more detailed report presented at the Brookhaven Symposium on Heavy Ion Physics From 10 to 200 MeV/A, July 16-20, 1979.

Table 1. Parameters of the K = 800 spectrograph.

Energy resolution:	$\Delta E/E = 10^{-4}$ @ 1 mm radial target spot size
Energy range:	$\Delta E/E = 10\%$
Solid angle:	$\Omega = 5 \times 10^{-3}$ sr
Resolving power:	$D/M = 21$
Radial dispersion:	$D = 7$ cm/%
Axial dispersion:	$R_{34} = 0.7$ mm/mr
Radial magnification:	$M = 0.33$
Angular resolution:	$\Delta\theta \lesssim 2$ mr (total of beam plus spectrograph contribution)
Focal plane size:	40 cm radial x 10 cm axial
Focal plant tilt:	10° from normal incidence
Magnetic rigidity:	$B\rho = 4$ T-m
Dipole fields:	$B = 1.5$ T ($\rho = 2.7$ m)
Dipole gap:	$d = 6$ cm
Dipole sizes:	#1 3.5 m long x 50 cm wide (75° bend) #2 4.0 m long x 75 cm wide (86° bend)
Weight of dipoles:	#1 50 tons #2 100 tons
Quadrupole sizes:	15 cm ID x 40 cm long

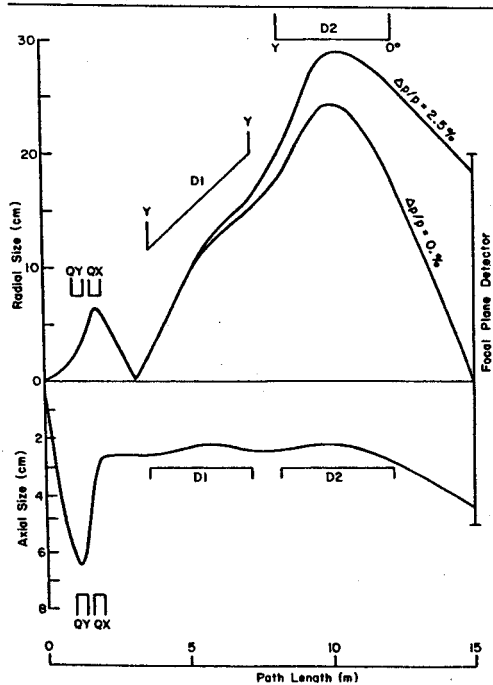


Fig. 4. Plots of the radial and axial beam envelopes of the proposed K = 800 spectrograph.

Status of the Reaction Product Mass Spectrograph
L. Harwood, J. Nolen, E. Kashy, R. Pardo, H. Enge*
*Massachusetts Institute of Technology

One of the major areas of use for any accelerator in the 10-200 MeV/nucleon energy range will be in production of new nuclei far from β -stability or in the "super heavy" mass region. A device which can measure the mass of these nuclei directly as they are emitted from the target would be extremely useful. During the past several months several designs for such a reaction product mass spectrograph (RPMS) to be used with the MSU super-conducting cyclotrons have been studied. The following gives the details of the current plans of a system which appears potentially useful over a wide (1-200 MeV/nucleon) energy range.

Unlike the MIT-BNL¹ Energy - Mass Spectrometer (EMS), we feel the best design is one which has a mass focal plane, ie a device that focusses all particles of a given M/q onto a spot on the focal plane independent of the energies of the particles. This can be accomplished by appropriate combinations of devices that disperse according to energy, velocity, and momentum to yield a composite that disperses according to mass. The devices available are electric septums, Wien filters, and magnetic dipoles; a combination of any different two of the above devices could yield a device which disperses according to M/q only.

From monetary considerations, it would be best if the same elements could be used to build a mass spectrograph useful over the full energy range of the MSU Phase II facility. This constraint rules out electric septums since the limit on attainable field gradients (≈ 80 kV/cm with a 10 cm gap) would require a 50 m radius of curvature for the 200 MeV/nucleon particles available from Phase II. A 5 m length is necessary to achieve a reasonable mass resolution ($\approx 1\%$) with reasonable solid angle (≈ 1 msr) at 200 MeV/A. Because the curvature of the septum is determined by the maximum energy particles and the maximum electric field, this device would not be optimized for lower energies, where larger resolving powers are possible. One would thus need separate septums for low energies (≈ 20 MeV/nucleon) and high energies (≈ 150 MeV/nucleon). Construction of either of the two septums would be a costly, time consuming project in itself. We have chosen instead to use one of the Mark VI 15-foot velocity separators used previously in the high energy physics program at the Bevatron. One of these separators has been obtained and is at MSU. The advantages of this device are that since the electrostatic plates are straight, it is effective over the entire energy range of interest (1 MeV/A

to 200 MeV/A) and that its dispersive capabilities match the experiments of interest at the different energies.

The design for the entire system currently under consideration is shown in Fig. 1. The design might appear excessive with its 12 multipoles, but these multipoles are necessary to make possible the correction of the large number of second-order aberrations.

For Phase I operation (up to 80 MeV/A) overall length is 18.5 m. The layout will be larger for Phase II (up to 200 MeV/A) because of the quadrupole focussing limitations. Since such a long device would be exceedingly difficult to move from angle to angle, we intend to change the angle of incidence of the beam rather than moving the spectrometer. This can be accomplished for a span of 30° by using a pair of small superconducting dipoles. A single larger angle, such as 60° , might be obtained by inflection from the adjacent beam line.

The multipoles are arranged as four triplets. Each multipole will be a combined quadrupole, sextupole, and octupole, with each $2n$ -pole component being independently variable. As stated above, the multipoles will be superconducting. We are considering the Panofsky² design as it provides high quality fields without elaborate construction procedures. The variable octupole components are produced by the same coils as produce the variable quadrupole components, an added benefit of the Panofsky design. The specific design for the sextupoles has not been decided at this time. We should be able to correct most of the second-order aberrations and several of the third order aberrations, our aim being line widths of about 1 mm.

The optics calculations have been done with the computer code TRANSPORT.⁴ This is a first and second order matrix multiplication program. All of the standard magnetic devices (quadrupoles, dipoles, etc.) are included in the program; Wien filters are not. The matrices for the Wien filter are calculated from the equations given by Ioaniviciu.⁵ These matrices are then input into TRANSPORT where necessary.

The first order optics have been designed to facilitate correction of second order aberrations. Some of the rays are illustrated in Fig. 1. Note that there is a horizontal cross-over after the first triplet following the Wien filter. A velocity focal plane exists at this point. Thus a crude velocity selection can be made by introducing a set of slits which pass the desired range of velocities and prevent others from

continuing to the mass focal plane.

At present, second order calculations continue. A 2 mm wide line width has already been attained for 3 msr solid angle. As the calculations continue, details of the optics may change. The present first order characteristics are given in Table I.

Table I. RPMS Specifications (as of 7/11/79).

Solid angle: $\Omega = 1$ msr
Mass dispersion/magnification (D/M) = 0.47 cm/percent
Length: 18.5 meters
Multipoles: superconducting; combined 4-, 6-, and 8-pole
Wien filter: length 5 meters, gap 10 cm, ± 150 kV, 470 Gauss
Second order line width (at 1 msr and $\pm 5\%$ velocity and mass range): 2 mm
Particle used in calculations: 20 MeV/nucleon, $A = 2Z$, fully stripped

Fig. 2 shows the mass resolving power over a range of energies. At 200 MeV/nucleon, D/M is still about $1 \text{ mm}/\% \frac{\Delta m}{m}$. With a 1 mm line width, one could resolve masses 100 and 101, for example.

1. H.A. Enge, private communication.
2. L.N. Hand and W.K.H. Panofsky, Rev. Sci. Inst. 30, 927 (1959).
3. K.L. Brown, et al, SLAC report 91 (1973).
4. D. Ioanoviciu, Int. Journal of Mass Spect. and Ion Phys. 15.

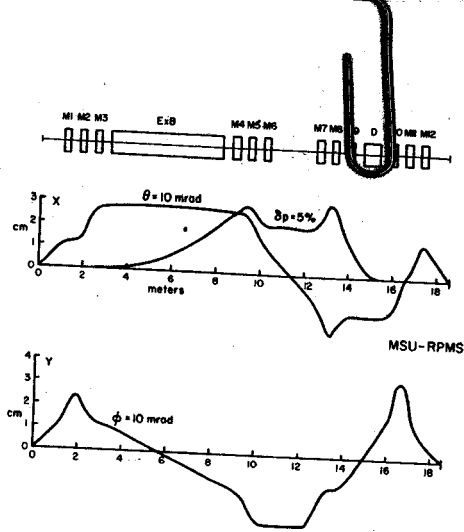


Fig. 1. Block diagram of RPMS with the x/θ , x/δ , and y/ϕ rays indicated. "M" indicates a multipole focussing element, "ExB" the Wien filter, and "D" the magnetic dipole.

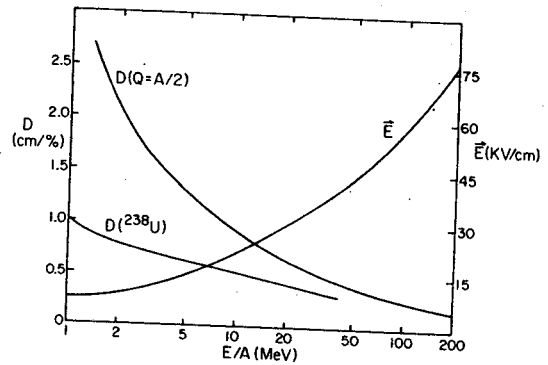


Fig. 2. Dispersion possible with the Mark VI Wien filter. These calculations are for the magnetic field limit of 470 Gauss. The magnification of the system is unity for all calculations and the solid angle is roughly constant over the energy range.